Measurement of J/ψ at forward and backward rapidity in p+p, p+Al, p+Au, and ^{3}He+Au collisions at $\sqrt{s_{NN}} = 200$ GeV

A. Adare,[12] C. Aidala,[41] N.N. Ajitanand,[57,*] Y. Akiba,[52,53,†] M. Alfred,[22] V. Andrieux,[41] N. Apadula,[27,58] H. Asano,[34,52] B. Azmoun,[7] V. Babintsev,[23] M. Bai,[6] N.S. Bandara,[40] B. Bannier,[58] K.N. Barish,[8] S. Bathe,[5,53] A. Bazilevsky,[7] M. Beaumier,[8] S. Beckman,[12] R. Belmont,[12,41] A. Berdnikov,[55] Y. Berdnikov,[55] D.S. Blau,[33,44] M. Boer,[36] J.S. Bok,[46] K. Boyle,[53] M.L. Brooks,[36] J. Bryslawskyj,[5,8] V. Bumazhnov,[23] S. Campbell,[13,27] V. Canoa Roman,[58] R. Cervantes,[58] C.-H. Chen,[53] C.Y. Chi,[13] M. Chiu,[7] I.J. Choi,[24] J.B. Choi,[29,*] T. Chujo,[61] Z. Citron,[63] M. Connors,[20,53] N. Cronin,[42,58] M. Csanád,[16] T. Csörgő,[17,64] T.W. Danley,[47] A. Datta,[45] M.S. Daugherity,[1] G. David,[7,15,58] K. DeBlasio,[45] K. Dehmelt,[58] A. Denisov,[23] A. Deshpande,[7,53,58] E.J. Desmond,[7] A. Dion,[58] P.B. Diss,[39] D. Dixit,[58] J.H. Do,[65] A. Drees,[58] K.A. Drees,[6] J.M. Durham,[36] A. Durum,[23] A. Enokizono,[52,54] H. En'yo,[52] S. Esumi,[61] B. Fadem,[42] W. Fan,[58] N. Feege,[58] D.E. Fields,[45] M. Finger,[9] M. Finger, Jr.,[9] S.L. Fokin,[33] J.E. Frantz,[47] A. Franz,[7] A.D. Frawley,[19] Y. Fukuda,[61] C. Gal,[58] P. Gallus,[14] P. Garg,[3,58] H. Ge,[58] F. Giordano,[24] A. Glenn,[35] Y. Goto,[52,53] N. Grau,[2] S.V. Greene,[62] M. Grosse Perdekamp,[24] T. Gunji,[11] H. Guragain,[20] T. Hachiya,[43,52,53] J.S. Haggerty,[7] K.I. Hahn,[18] H. Hamagaki,[11] H.F. Hamilton,[1] S.Y. Han,[18,52] J. Hanks,[58] S. Hasegawa,[28] T.O.S. Haseler,[20] K. Hashimoto,[52,54] X. He,[20] T.K. Hemmick,[58] J.C. Hill,[27] K. Hill,[12] A. Hodges,[20] R.S. Hollis,[8] K. Homma,[21] B. Hong,[32] T. Hoshino,[21] N. Hotvedt,[27] J. Huang,[7] S. Huang,[62] K. Imai,[28] M. Inaba,[61] A. Iordanova,[8] D. Isenhower,[1] D. Ivanishchev,[51] B.V. Jacak,[58] M. Jezghani,[20] Z. Ji,[58] J. Jia,[7,57] X. Jiang,[36] B.M. Johnson,[7,20] D. Jouan,[49] D.S. Jumper,[24] S. Kanda,[11] J.H. Kang,[65] D. Kapukchyan,[8] S. Karthas,[58] D. Kawall,[40] A.V. Kazantsev,[33] J.A. Key,[45] V. Khachatryan,[58] A. Khanzadeev,[51] C. Kim,[8,32] D.J. Kim,[30] E.-J. Kim,[29] G.W. Kim,[18] M. Kim,[52,56] B. Kimelman,[42] D. Kincses,[16] E. Kistenev,[7] R. Kitamura,[11] J. Klatsky,[19] D. Kleinjan,[8] P. Kline,[58] T. Koblesky,[12] B. Komkov,[51] D. Kotov,[51,55] S. Kudo,[61] B. Kurgyis,[16] K. Kurita,[54] M. Kurosawa,[52,53] Y. Kwon,[65] R. Lacey,[57] J.G. Lajoie,[27] A. Lebedev,[27] S. Lee,[65] S.H. Lee,[27,58] M.J. Leitch,[36] Y.H. Leung,[58] N.A. Lewis,[41] X. Li,[10] X. Li,[36] S.H. Lim,[36,65] M.X. Liu,[36] V.-R. Loggins,[24] S. Lökös,[16,17] K. Lovasz,[15] D. Lynch,[7] T. Majoros,[15] Y.I. Makdisi,[6] M. Makek,[66] A. Manion,[58] V.I. Manko,[33] E. Mannel,[7] M. McCumber,[36] P.L. McGaughey,[36] D. McGlinchey,[12,36] C. McKinney,[24] A. Meles,[46] M. Mendoza,[8] W.J. Metzger,[17] A.C. Mignerey,[39] D.E. Mihalik,[58] A. Milov,[63] D.K. Mishra,[4] J.T. Mitchell,[7] Iu. Mitrankov,[55] G. Mitsuka,[31,52,53] S. Miyasaka,[52,60] S. Mizuno,[52,61] A.K. Mohanty,[4] P. Montuenga,[24] T. Moon,[65] D.P. Morrison,[7] S.I. Morrow,[62] T.V. Moukhanova,[33] T. Murakami,[34,52] J. Murata,[52,54] A. Mwai,[57] K. Nagai,[60] K. Nagashima,[21,52] T. Nagashima,[54] J.L. Nagle,[12] M.I. Nagy,[16] I. Nakagawa,[52,53] H. Nakagomi,[52,61] K. Nakano,[52,60] C. Nattrass,[59] P.K. Netrakanti,[4] T. Niida,[61] S. Nishimura,[11] R. Nishitani,[43] R. Nouicer,[7,53] T. Novák,[17,64] N. Novitzky,[30,58] A.S. Nyanin,[33] E. O'Brien,[7] C.A. Ogilvie,[27] J.D. Orjuela Koop,[12] J.D. Osborn,[41] A. Oskarsson,[37] G.J. Ottino,[45] K. Ozawa,[31,61] R. Pak,[7] V. Pantuev,[25] V. Papavassiliou,[46] J.S. Park,[56] S. Park,[52,56,58] S.F. Pate,[46] M. Patel,[27] J.-C. Peng,[24] W. Peng,[62] D.V. Perepelitsa,[7,12] G.D.N. Perera,[46] D.Yu. Peressounko,[33] C.E. PerezLara,[58] J. Perry,[27] R. Petti,[7,58] M. Phipps,[7,24] C. Pinkenburg,[7] R. Pinson,[1] R.P. Pisani,[7] A. Pun,[47] M.L. Purschke,[7] P.V. Radzevich,[55] J. Rak,[30] B.J. Ramson,[41] I. Ravinovich,[63] K.F. Read,[48,59] D. Reynolds,[57] V. Riabov,[44,51] Y. Riabov,[51,55] D. Richford,[5] T. Rinn,[27] S.D. Rolnick,[8] M. Rosati,[27] Z. Rowan,[5] J.G. Rubin,[41] J. Runchey,[27] A.S. Safonov,[55] B. Sahlmueller,[58] N. Saito,[31] T. Sakaguchi,[7] H. Sako,[28] V. Samsonov,[44,51] M. Sarsour,[20] S. Sato,[28] B. Schaefer,[62] B.K. Schmoll,[59] K. Sedgwick,[8] R. Seidl,[52,53] A. Sen,[27,59] R. Seto,[8] P. Sett,[4] A. Sexton,[39] D. Sharma,[58] I. Shein,[23] T.-A. Shibata,[52,60] K. Shigaki,[21] M. Shimomura,[27,43] T. Shioya,[61] P. Shukla,[4] A. Sickles,[7,24] C.L. Silva,[36] D. Silvermyr,[37,48] B.K. Singh,[3] C.P. Singh,[3] V. Singh,[3] M.J. Skoby,[41] M. Slunečka,[9] K.L. Smith,[19] M. Snowball,[36] R.A. Soltz,[35] W.E. Sondheim,[36] S.P. Sorensen,[59] I.V. Sourikova,[7] P.W. Stankus,[48] M. Stepanov,[40,*] S.P. Stoll,[7] T. Sugitate,[21] A. Sukhanov,[7] T. Sumita,[52] J. Sun,[58] Z. Sun,[15] S. Suzuki,[43] J. Sziklai,[64] A. Taketani,[52,53] K. Tanida,[28,53,56] M.J. Tannenbaum,[7] S. Tarafdar,[62,63] A. Taranenko,[44,57] G. Tarnai,[15] R. Tieulent,[20,38] A. Timilsina,[27] T. Todoroki,[52,53,61] M. Tomášek,[14] C.L. Towell,[1] R. Towell,[1] R.S. Towell,[1] I. Tserruya,[63] Y. Ueda,[21] B. Ujvari,[15] H.W. van Hecke,[36] J. Velkovska,[62] M. Virius,[14] V. Vrba,[14,26] N. Vukman,[66] X.R. Wang,[46,53] Z. Wang,[5] Y. Watanabe,[52,53] Y.S. Watanabe,[11,31] F. Wei,[46] A.S. White,[41] C.P. Wong,[20] C.L. Woody,[7] M. Wysocki,[48] B. Xia,[47] C. Xu,[46] Q. Xu,[62] L. Xue,[20] S. Yalcin,[58] Y.L. Yamaguchi,[11,53,58] H. Yamamoto,[61] A. Yanovich,[23] J.H. Yoo,[32,53] I. Yoon,[56] H. Yu,[46,50] I.E. Yushmanov,[33] W.A. Zajc,[13] A. Zelenski,[6] S. Zharko,[55] S. Zhou,[10] and L. Zou[8]

(PHENIX Collaboration)

[1] *Abilene Christian University, Abilene, Texas 79699, USA*

[2] *Department of Physics, Augustana University, Sioux Falls, South Dakota 57197, USA*

[3]*Department of Physics, Banaras Hindu University, Varanasi 221005, India*
[4]*Bhabha Atomic Research Centre, Bombay 400 085, India*
[5]*Baruch College, City University of New York, New York, New York, 10010 USA*
[6]*Collider-Accelerator Department, Brookhaven National Laboratory, Upton, New York 11973-5000, USA*
[7]*Physics Department, Brookhaven National Laboratory, Upton, New York 11973-5000, USA*
[8]*University of California-Riverside, Riverside, California 92521, USA*
[9]*Charles University, Ovocný trh 5, Praha 1, 116 36, Prague, Czech Republic*
[10]*Science and Technology on Nuclear Data Laboratory, China Institute of Atomic Energy, Beijing 102413, People's Republic of China*
[11]*Center for Nuclear Study, Graduate School of Science, University of Tokyo, 7-3-1 Hongo, Bunkyo, Tokyo 113-0033, Japan*
[12]*University of Colorado, Boulder, Colorado 80309, USA*
[13]*Columbia University, New York, New York 10027 and Nevis Laboratories, Irvington, New York 10533, USA*
[14]*Czech Technical University, Zikova 4, 166 36 Prague 6, Czech Republic*
[15]*Debrecen University, H-4010 Debrecen, Egyetem tér 1, Hungary*
[16]*ELTE, Eötvös Loránd University, H-1117 Budapest, Pázmány P. s. 1/A, Hungary*
[17]*Eszterházy Károly University, Károly Róbert Campus, H-3200 Gyöngyös, Mátrai út 36, Hungary*
[18]*Ewha Womans University, Seoul 120-750, Korea*
[19]*Florida State University, Tallahassee, Florida 32306, USA*
[20]*Georgia State University, Atlanta, Georgia 30303, USA*
[21]*Hiroshima University, Kagamiyama, Higashi-Hiroshima 739-8526, Japan*
[22]*Department of Physics and Astronomy, Howard University, Washington, DC 20059, USA*
[23]*IHEP Protvino, State Research Center of Russian Federation, Institute for High Energy Physics, Protvino, 142281, Russia*
[24]*University of Illinois at Urbana-Champaign, Urbana, Illinois 61801, USA*
[25]*Institute for Nuclear Research of the Russian Academy of Sciences, prospekt 60-letiya Oktyabrya 7a, Moscow 117312, Russia*
[26]*Institute of Physics, Academy of Sciences of the Czech Republic, Na Slovance 2, 182 21 Prague 8, Czech Republic*
[27]*Iowa State University, Ames, Iowa 50011, USA*
[28]*Advanced Science Research Center, Japan Atomic Energy Agency, 2-4 Shirakata Shirane, Tokai-mura, Naka-gun, Ibaraki-ken 319-1195, Japan*
[29]*Jeonbuk National University, Jeonju, 54896, Korea*
[30]*Helsinki Institute of Physics and University of Jyväskylä, P.O.Box 35, FI-40014 Jyväskylä, Finland*
[31]*KEK, High Energy Accelerator Research Organization, Tsukuba, Ibaraki 305-0801, Japan*
[32]*Korea University, Seoul, 02841*
[33]*National Research Center "Kurchatov Institute", Moscow, 123098 Russia*
[34]*Kyoto University, Kyoto 606-8502, Japan*
[35]*Lawrence Livermore National Laboratory, Livermore, California 94550, USA*
[36]*Los Alamos National Laboratory, Los Alamos, New Mexico 87545, USA*
[37]*Department of Physics, Lund University, Box 118, SE-221 00 Lund, Sweden*
[38]*IPNL, CNRS/IN2P3, Univ Lyon, Universit Lyon 1, F-69622, Villeurbanne, France*
[39]*University of Maryland, College Park, Maryland 20742, USA*
[40]*Department of Physics, University of Massachusetts, Amherst, Massachusetts 01003-9337, USA*
[41]*Department of Physics, University of Michigan, Ann Arbor, Michigan 48109-1040, USA*
[42]*Muhlenberg College, Allentown, Pennsylvania 18104-5586, USA*
[43]*Nara Women's University, Kita-uoya Nishi-machi Nara 630-8506, Japan*
[44]*National Research Nuclear University, MEPhI, Moscow Engineering Physics Institute, Moscow, 115409, Russia*
[45]*University of New Mexico, Albuquerque, New Mexico 87131, USA*
[46]*New Mexico State University, Las Cruces, New Mexico 88003, USA*
[47]*Department of Physics and Astronomy, Ohio University, Athens, Ohio 45701, USA*
[48]*Oak Ridge National Laboratory, Oak Ridge, Tennessee 37831, USA*
[49]*IPN-Orsay, Univ. Paris-Sud, CNRS/IN2P3, Université Paris-Saclay, BP1, F-91406, Orsay, France*
[50]*Peking University, Beijing 100871, People's Republic of China*
[51]*PNPI, Petersburg Nuclear Physics Institute, Gatchina, Leningrad region, 188300, Russia*
[52]*RIKEN Nishina Center for Accelerator-Based Science, Wako, Saitama 351-0198, Japan*
[53]*RIKEN BNL Research Center, Brookhaven National Laboratory, Upton, New York 11973-5000, USA*
[54]*Physics Department, Rikkyo University, 3-34-1 Nishi-Ikebukuro, Toshima, Tokyo 171-8501, Japan*
[55]*Saint Petersburg State Polytechnic University, St. Petersburg, 195251 Russia*
[56]*Department of Physics and Astronomy, Seoul National University, Seoul 151-742, Korea*
[57]*Chemistry Department, Stony Brook University, SUNY, Stony Brook, New York 11794-3400, USA*
[58]*Department of Physics and Astronomy, Stony Brook University, SUNY, Stony Brook, New York 11794-3800, USA*
[59]*University of Tennessee, Knoxville, Tennessee 37996, USA*
[60]*Department of Physics, Tokyo Institute of Technology, Oh-okayama, Meguro, Tokyo 152-8551, Japan*
[61]*Tomonaga Center for the History of the Universe, University of Tsukuba, Tsukuba, Ibaraki 305, Japan*
[62]*Vanderbilt University, Nashville, Tennessee 37235, USA*
[63]*Weizmann Institute, Rehovot 76100, Israel*

[64] *Institute for Particle and Nuclear Physics, Wigner Research Centre for Physics, Hungarian Academy of Sciences (Wigner RCP, RMKI) H-1525 Budapest 114, POBox 49, Budapest, Hungary*
[65] *Yonsei University, IPAP, Seoul 120-749, Korea*
[66] *Department of Physics, Faculty of Science, University of Zagreb, Bijenička c. 32 HR-10002 Zagreb, Croatia*
(Dated: October 29, 2019)

Charmonium is a valuable probe in heavy-ion collisions to study the properties of the quark gluon plasma, and is also an interesting probe in small collision systems to study cold nuclear matter effects, which are also present in large collision systems. With the recent observations of collective behavior of produced particles in small system collisions, measurements of the modification of charmonium in small systems have become increasingly relevant. We present the results of J/ψ measurements at forward and backward rapidity in various small collision systems, p+p, p+Al, p+Au and ^{3}He+Au, at $\sqrt{s_{NN}}$=200 GeV. The results are presented in the form of the observable R_{AB}, the nuclear modification factor, a measure of the ratio of the J/ψ invariant yield compared to the scaled yield in p+p collisions. We examine the rapidity, transverse momentum, and collision centrality dependence of nuclear effects on J/ψ production with different projectile sizes p and ^{3}He, and different target sizes Al and Au. The modification is found to be strongly dependent on the target size, but to be very similar for p+Au and ^{3}He+Au. However, for ~~0–20%~~0%–20% central collisions at backward rapidity, the modification for ^{3}He+Au is found to be smaller than that for p+Au, with a mean fit to the ratio of $0.89 \pm 0.03(\text{stat}) \pm 0.08(\text{syst})$, possibly indicating final state effects due to the larger projectile size.

I. INTRODUCTION

The cross section for production of charmonium in proton collisions with heavy nuclei is strongly modified relative to that in p+p collisions. The effects that cause this modification are often referred to as cold nuclear matter (CNM) effects because of the long-time presumption that the energy density and temperature produced in the collision of a single proton with a nucleus were not sufficient to form a deconfined quark-gluon plasma. The CNM effects that can modify charm production in p+A collisions include modification of the nuclear-parton-distribution functions (nPDFs) in a nucleus [**?** **?**], initial state parton energy loss [**?**], breakup of the forming charmonium in collisions with target nucleons [**?** **?**], coherent gluon saturation [**?** **?**], and transverse momentum broadening [**?**]. These mechanisms are generally expected to act in the early stages of the collision, and effect either the production rates of charm quarks or their propagation through the nucleus. All of these processes are strongly (and differently) dependent on the rapidity and transverse momentum of the produced charmonium, and the collision energy. They are therefore best studied using p+A data covering the broadest possible range of collision energy, rapidity and transverse momentum.

At the Relativistic Heavy Ion Collider (RHIC) p+p, d+Au, p+Au, ^{3}He+Au and p+Al collisions have been studied at $\sqrt{s_{NN}} = 200$ GeV. The PHENIX experiment published data on J/ψ production in d+Au collisions over the rapidity intervals $1.2 < |y| < 2.2$ and $|y| < 0.35$ [**?** **?**]. PHENIX also reported measurements of the $\psi(2S)$ in small collision systems, first with nuclear modification in d+Au collisions ($|y| < 0.35$) [**?**], followed by ~~$\psi(2S)/J/\psi$ ratio measurements~~ measurements of the ratio of $\psi(2S)$ to J/ψ in p+Al, p+Au and ^{3}He+Au collisions at $\sqrt{s_{NN}} = 200$ GeV ($1.2 < |y| < 2.2$) [**?**]. STAR has reported J/ψ data for d+Au collisions [**?**] ($|y| < 1$).

At the Large Hadron Collider (LHC) p+Pb collisions have been studied at $\sqrt{s} = 5.02$ TeV. ALICE has reported data for J/ψ [**?** **?**] and $\psi(2S)$ [**?** **?**] ($-4.46 < y < -2.96$ and $2.03 < y < 3.53$). LHCb has reported $\psi(2S)$ data [**?**] ($-5.0 < y < -2.5$ and $1.5 < y < 4.0$). CMS has reported J/ψ [**?**] and $\psi(2S)$ [**?**] data ($-2.4 < y < 1.93$ and $p_T > 4$ GeV/c). ATLAS has reported J/ψ [**?**] and charmonium [**?**] data ($|y| < 2$ and $p_T > 8$ GeV/c). These measurements show a significant energy, rapidity and p_T dependence of the modification of charmonia production compared to the scaled p+p results.

The assumption that effects due to soft particles produced in the collision are not important in p or d+A collision at colliders was called into question by the observation of strong suppression of the $\psi(2S)$ relative to the J/ψ in central d+Au collisions [**?**], and then in p+Pb collisions [**?**]. Because CNM effects on the production of charm quarks and their transport through the nucleus are expected to affect both states similarly, they do not appear to be able to explain this observation. However, it can be reproduced by the co-mover break up model [**?**], where charmonium is dissociated by interactions with produced particles in the final state, which naturally gives a larger suppression effect on the much more weakly bound $\psi(2S)$. The observation of flow-like behavior in p+Pb collisions at LHC (see for example [**?**]) and later in d+Au collisions at RHIC [**?** **?**] suggested that a quark-gluon plasma of small size may be formed in high energy collisions of these light systems. This led to the application of transport models to p+Pb and d+Au data, which were originally developed for charmonium production in heavy ion collisions [**?** **?**]. A plasma

* Deceased
† PHENIX Spokesperson: akiba@rcf.rhic.bnl.gov

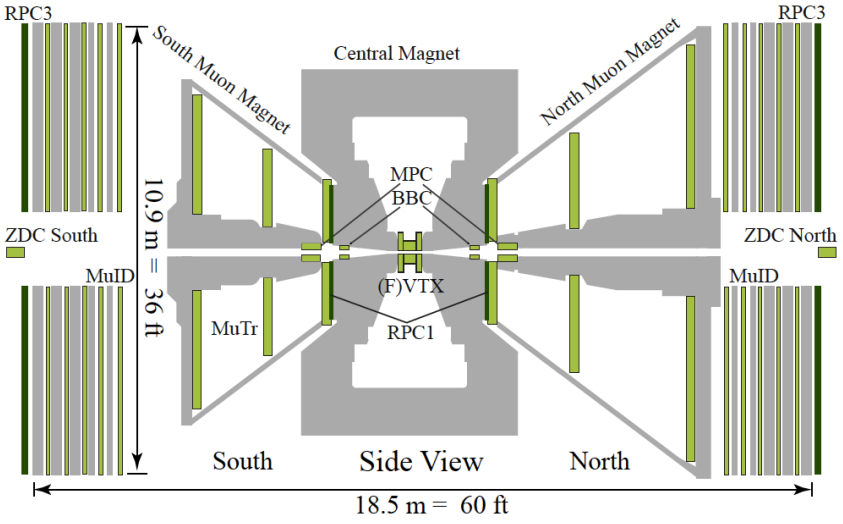

FIG. 1. Side view of the PHENIX detector in 2014 and 2015.

phase in these small collision systems gives different suppression between the charmonia states and allows a description of the data. In the case of most central midrapidity d+Au collisions at $\sqrt{s_{NN}} = 200$ GeV, additional suppression beyond CNM effects has been predicted of approximately 20% for the J/ψ, and 55% for the $\psi(2S)$ [**?**], in good agreement with the data [**? ?**].

In 2014 and 2015, the Relativistic Heavy Ion Collider (RHIC) provided collisions of p+Al, p+Au and ^{3}He+Au for a systematic study of small systems. A comparison of flow data from p+Au, d+Au and ^{3}He+Au with hydrodynamic models found that the data were all consistent with hydrodynamic flow in the most central collisions [**? ? ?**]. An obvious question is whether increased energy density provided by the ^{3}He projectile in comparison to the proton produces any observable effect on charmonium modification in collisions with a Au target.

In this paper we present PHENIX measurements of inclusive J/ψ production in p+Al, p+Au and ^{3}He+Au collisions at $\sqrt{s_{NN}} = 200$ GeV. The inclusive J/ψ cross section includes feed-down from $\psi(2s2S)$ and χ_c states, and a smaller contribution from B-meson decays. The results are directly compared to p+p collisions at the same center of mass energy by calculating the nuclear modification factor R_{AB}. The data are presented as a function of J/ψ p_T, rapidity, and centrality, and compared to theoretical models.

II. EXPERIMENTAL SETUP

The PHENIX detector [**?**] comprises two central arm spectrometers at midrapidity and two muon arm spectrometers at forward and backward rapidity. The detector configuration during the data taking in 2014 and 2015 is shown in Fig. 1. The data presented here are from $J/\psi \to \mu^+\mu^-$ decays recorded with the muon arm spectrometers. The muon spectrometers have full azimuthal acceptance, covering $-2.2 < \eta < -1.2$ (south arm) and $1.2 < \eta < 2.4$ (north arm). Each muon arm comprises a Forward Silicon Vertex Tracker (FVTX), followed by a hadron absorber and a muon spectrometer.

The FVTX [**?**] is a silicon detector designed to measure a precise collision vertex (also constrained by the Silicon Vertex Tracker (VTX) at midrapidity), and to provide precise tracking for charged particles entering the muon spectrometer before undergoing multiple scattering in the hadron absorber. The FVTX was not used in this inclusive J/ψ analysis, because the acceptance is reduced when requiring muon arm tracks that match tracks in the FVTX. Following the FVTX is the hadron absorber, composed of layers of copper, iron, and stainless steel, corresponding to 7.2 nuclear interaction lengths (λ_I). The absorber suppresses hadrons in front of the muon arm by a factor of approximately 1000, thus significantly reducing hadronic background for muon based measurements.

Each of the muon spectrometers is composed of a muon tracker (MuTr) embedded in a magnetic field followed by a muon identifier (MuID). Each MuTr comprises three stations of cathode strip chambers, inside a magnet with a radial field integral of $\int \mathrm{B} \cdot dl = 0.72$ T $\cdot$ m. It provides a momentum measurement for charged particles. Each MuID is composed of five layers (referred to as gap 0–4) of steel absorber (4.8 (5.4) λ_I for south (north) arm) and two planes of Iarocci tubes. This enables the separation of muons and hadrons based on their penetration depth at a given reconstructed momentum. The MuID in each arm is also used to trigger events containing two or more muon tracks per event, called a dimuon trigger, and each muon track is required to have at least one hit in either gap 3 or gap 4. A more detailed discussion of the PHENIX muon arms can be found in Ref. [**? ?**].

The beam-beam counters (BBC) are used to determine

the collision vertex position along the beam axis ($z_{\rm BBC}$) with a resolution of roughly 2 cm in p+p collisions. Each BBC comprises two arrays of 64 quartz Čerenkov detectors located at $z = \pm 144$ cm from the nominal interaction point, and has an acceptance covering the full azimuth and $3.1 < |\eta| < 3.9$. They also provide a minimum bias (MB) trigger by requiring at least one hit in each BBC. The BBC trigger efficiency, determined from the Van der Meer scan technique [**?**], is 55% ±5% for inelastic p+p events and 79% ± 2% for events with midrapidity particle production [**?** **?**]. In p+Al, p+Au, and ^{3}He+Au collisions, charged particle multiplicity in the BBC in the Au/Al-going direction ($-3.9 < \eta < -3.1$) is used to categorize the event centrality. The BBC trigger efficiency is 72% ± 4%, 84% ± 3%, and 88% ± 4% of inelastic p+Al, p+Au, and ^{3}He+Au collisions, respectively.

A Glauber model, combined with a simulation of the BBC response, is used to relate charged particle multiplicity in the BBC to parameters that characterize the collision centrality, as described in [**?**]. The analysis produces the average number of nucleon-nucleon collisions in each centrality category. It also produces centrality dependent BBC bias correction factors which account for the correlation between BBC charge and the presence of a hard scattering in the event, and are applied as a multiplicative correction on invariant yields. Table I shows the values of $\langle N_{coll}\rangle$ and BBC bias correction factor from this analysis.

TABLE I. $\langle N_{coll}\rangle$ and BBC bias correction factors for different centrality bins of p+Al, p+Au and ^{3}He+Au collisions.

Collision system	Centrality	$\langle N_{coll}\rangle$	Bias factor
p+Al	0%–20%	3.4±0.3	0.81±0.01
	20%–40%	2.4±0.1	0.90±0.02
	40%–72%	1.7±0.1	1.04±0.04
	0%–100%	2.1±0.1	0.80±0.02
p+Au	0%–5%	9.7±0.6	0.86±0.01
	5%–10%	8.4±0.6	0.90±0.01
	10%–20%	7.4±0.5	0.94±0.01
	20%–40%	6.1±0.4	0.98±0.01
	40%–60%	4.4±0.3	1.03±0.01
	60%–84%	2.6±0.2	1.00±0.06
	0%–100%	4.7±0.3	0.86±0.01
^{3}He+Au	0%–20%	22.3±1.7	0.95±0.01
	20%–40%	14.8±1.1	0.95±0.01
	40%–88%	5.5±0.4	1.03±0.01
	0%–100%	10.4±0.7	0.89±0.01

III. DATA ANALYSIS

A. Data set

The data sets used in this analysis are ^{3}He+Au data collected in 2014, and p+p, p+Al, and p+Au data collected in 2015. All data sets were recorded at a center of mass energy $\sqrt{s_{NN}}$=200 GeV. The events considered here are triggered by the dimuon trigger and are required to have a vertex within ±30 cm of the center of the interaction region. The corresponding integrated luminosity is 47 pb^{-1} for p+p, 590 nb^{-1} for p+Al, 138 nb^{-1} for p+Au, and 18 nb^{-1} for ^{3}He+Au collisions.

B. J/ψ signal extraction

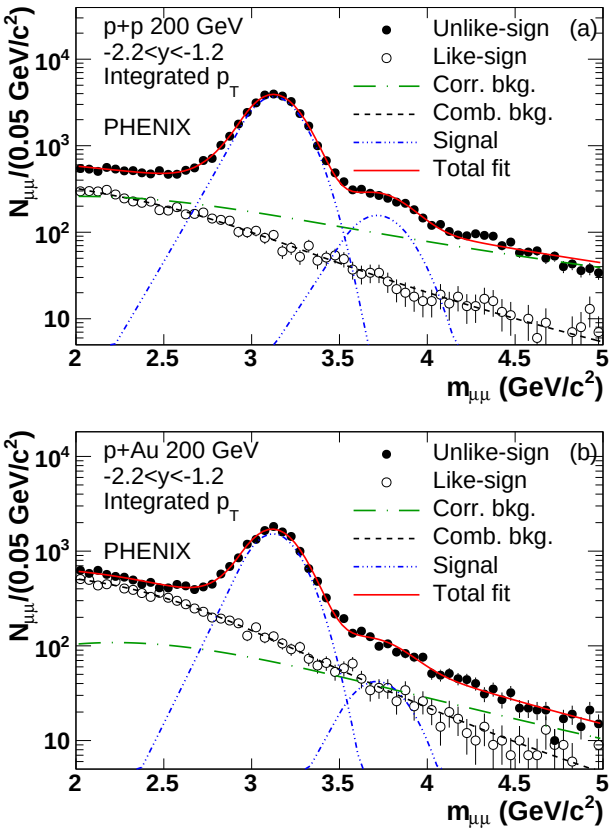

FIG. 2. Invariant mass distributions of unlike-sign and like-sign dimuons in MB p+p and p+Au collisions in the south muon arm. Fit results to extract the J/ψ signal are also presented.

Yields of J/ψ mesons were extracted from the invariant mass spectra constructed from combinations of unlike-sign tracks that are identified as muons. The mass spectra contain muon pairs from J/ψ decays, as well as significant contributions from combinations of real muons not from a J/ψ, as well as misidentified hadrons. Details about the dimuon selection to reduce the background contributions are described in [**?** **?**].

The mass spectrum constructed from like-sign tracks was used to estimate the background due to random combinations of kinematically unrelated tracks. A modified Hagedorn function was used to represent the correlated background due to kinematically related tracks. For J/ψ